Characterization of Self-Assembled Bilayers: Silver−Alkanethiolates

ARTICLE *in* LANGMUIR · OCTOBER 1998

Impact Factor: 4.46 · DOI: 10.1021/la980718g

5 AUTHORS, INCLUDING:

Erik Kruus
NEC Laboratories America
23 PUBLICATIONS **343** CITATIONS

SEE PROFILE

Characterization of self-assembled bilayers: silver-alkanethiolates

Bensebaa, Farid; Ellis, T.; Kruus, E.; Voicu, R.; Zhou, Y.

Publisher's version / la version de l'éditeur:
Langmuir, 14, 1998

Characterization of Self-Assembled Bilayers: Silver−Alkanethiolates

Farid Bensebaa,[†,§] Thomas H. Ellis,[*,†] Erik Kruus,[‡] Raluca Voicu,[†] and Yu Zhou[‡]

Département de chimie, Université de Montréal, Montréal, Québec, H3C 3J7, Canada, and Département de chimie, Université du Québec à Montréal, Montréal, Québec, H3C 3P8, Canada

Received June 17, 1998

Layered materials composed of silver−alkanethiolate units are characterized and compared to self-assembled alkanethiolate monolayers and thiolate-capped nanoparticles. A comprehensive infrared spectroscopy study is presented for silver−alkanethiolate materials having chain lengths varying from 7 to 18 carbon atoms (AgSC7 to AgSC18). The high level of definition in these spectra will make this a benchmark system for comparisons to other metal thiolate systems. An X-ray diffraction study of these same materials is used to determine the tilt angle of the chains (12 ± 3 °), which is very close to that reported for thiolate monolayers on Ag(111). These results are combined with a thorough characterization of the AgSC12 material using X-ray photoelectron spectroscopy, electronic spectroscopy, differential scanning calorimetry, and solid-state NMR. Overall, this provides a detailed description of the structure, the thermal stability, and the high degree of conformational order in these materials, which have not previously been extensively characterized at these chain lengths.

1. Introduction

Self-assembled monolayers (SAMs) composed of alkanethiolates are being extensively studied as a convenient means of functionalizing metal surfaces. Most work to date has been performed on flat gold surfaces, although a number of studies on silver surfaces have been reported.[1−9] Recently, it has been shown that thiolate-capped gold nanoparticles provide unique opportunities to provide insight into the properties of thiolate monolayers.[10−13] A recent report has shown that thiolate-capped silver nanoparticles can also be prepared.[14] Studies of nanoparticles are not limited to traditional surface science techniques, and this has provided a wealth of new information. It is now known that monolayers on both flat surfaces and on nanoparticles share many common properties. It is also known that the most important differences between the two systems can be accounted for because of the curvature of the nanoparticle surfaces, which creates microfacets with small domain sizes.

A second class of materials exists that shows great potential as a model system for SAM surfaces. These are layered materials that are composed of metal−alkanethiolate units,[15−17] whose structure is shown in Figure 1. Like SAMs on flat surfaces and on nanoparticles, these materials self-assemble in solution. The resulting multibilayer structure is clearly analogous to monolayers on flat surfaces: in fact it is the limit of an infinite surface-to-volume ratio. Unlike nanoparticles, there is no inherent surface curvature.

In the present work, the properties of silver−alkanethiolate layered materials will be presented, based on a wide range of measurements. The overall picture that emerges is that the layered systems are highly ordered, with the chain conformations being almost exclusively all-trans at room temperature. The ability to compare and contrast three different alkanethiolate self-assembled systems (bilayers, monolayers and nanoparticles) leads to a better understanding of the basic properties of all of these systems.

2. Experimental Section

Synthesis. Our two-phase method of preparation of the layered compounds differs slightly from previous methods.[15−17] The silver begins in the aqueous phase, in the form of silver nitrate. The alkanethiol (in slight excess) is dissolved in an organic solvent (toluene). When the two immiscible phases are brought into contact the silver−alkanethiolate forms near the interface as a solid suspension in the organic phase.

* To whom correspondence should be addressed.
† Université de Montréal.
‡ Université du Québec à Montréal.
§ Present address: ICPET, NRC of Canada, Ottawa, Ontario, Canada K1A 0R6.

(1) Walczak, M. M.; Chung, C.; Stole, S. M.; Widrig, C. A.; Porter, M. D. *J. Am. Chem. Soc.* **1991**, *113*, 2370−2378.
(2) Laibinis, P. E.; Whitesides, G. M.; Allara, D. L.; Tao, Y.-T.; Parikh, A. N.; Nuzzo, R. G. *J. Am. Chem. Soc.* **1991**, *113*, 7152−7167.
(3) Bryant, M. A.; Pemberton, J. E. *J. Am. Chem. Soc.* **1991**, *113*, 8284−8293.
(4) Fenter, P.; Eisenberger, P.; Li, J.; Camillone, N., III; Bernasek, S.; Scoles, G.; Ramanarayanan, T. A.; Liang, K. S. *Langmuir* **1991**, *7*, 2013−2016.
(5) Sellers, H.; Ulman, A.; Shnidman, Y.; Eilers, J. E. *J. Am. Chem. Soc.* **1993**, *115*, 9389−9401.
(6) Hines, M. A.; Todd, J. A.; Guyot-Sionnest, P. *Langmuir* **1995**, *11*, 493−497.
(7) Heinz, R.; Rabe, J. P. *Langmuir* **1995**, *11*, 506−511.
(8) Dhirani, A.; Hines, M. A.; Fisher, A. J.; Ismail, O.; Guyot-Sionnest, P. *Langmuir* **1995**, *11*, 2609−2614.
(9) Bensebaa, F.; Ellis, T. H.; Badia, A.; Lennox, R. B. *J. Vac. Sci. Technol. A* **1995**, *13*, 1331−1336.
(10) Brust, M.; Walker, M.; Bethell, D.; Schriffin, D. J.; Whyman, R. *J. Chem. Soc., Chem. Commun.* **1994**, 801−802.
(11) Hostetler, M. J.; Stokes, J. J.; Murray, R. W. *Langmuir* **1996**, *12*, 3604−3612.
(12) Weisbecker, C. S.; Merritt, M. V.; Whitesides, G. M. *Langmuir* **1996**, *12*, 3763−3772.
(13) Badia, A.; Cuccia, L.; Demers, L.; Morin, F.; Lennox, R. B. *J. Am. Chem. Soc.* **1997**, *119*, 2682−2692.
(14) Murthy, S.; Bigioni, T. P.; Wang, Z. L.; Khoury, J. T.; Whetten, R. L. *Mater. Lett.* **1997**, *30*, 321−325.
(15) Dance, I. G.; Fisher, K. J.; Banda, R. M. H.; Scudder, M. L. *Inorg. Chem.* **1991**, *30*, 183−187.
(16) Baena, M. J.; Espinet, P.; Lequerica, M. C.; Levelut, A. M. *J. Am. Chem. Soc.* **1992**, *114*, 4182−4185.
(17) Fijolek, H. G.; Grohal, J. R.; Sample, J. L.; Natan, M. J. *Inorg. Chem.* **1997**, *36*, 622−628.

10.1021/la980718g CCC: $15.00
Published on Web 10/06/1998

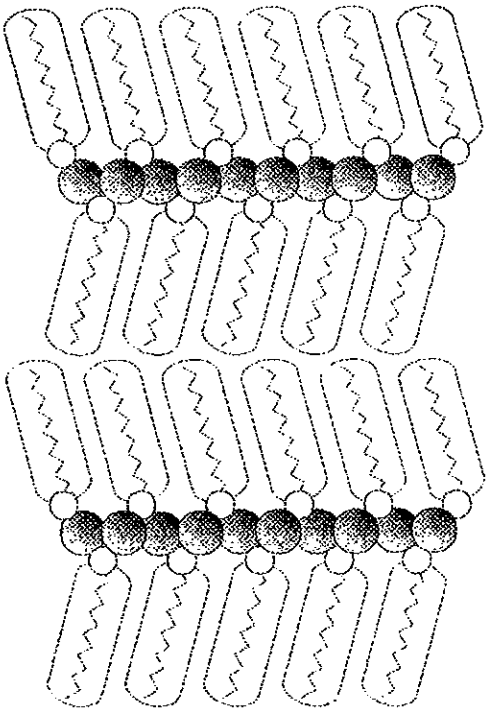

Figure 1. A schematic drawing of the layered structure of metal–alkanethiolate materials. The metal atoms are shaded circles, the sulfur atoms are white circles and the alkyl chains are represented by zigzag chains. The sizes are not to scale, but the tilt angle shown is close to that determined in this work. It is not known whether the metal atoms are confined to a plane as shown in the drawing.

The reaction can be written as follows:

$$AgNO_3(aq) + HS(CH_2)_nCH_3(org) \rightarrow HNO_3(aq) + AgS(CH_2)_nCH_3(org)$$

The exchange between the proton from the alkanethiol and the silver ion is confirmed by an analysis of the aqueous phase after the completion of the reaction. The pH of this phase is greatly diminished and no silver can be detected via precipitation with Cl^-. The overall yields are in excess of 90%.

The two phases are then separated; the organic phase is washed several times with water and the suspension is collected by centrifuging. The resulting white powders are washed several times with toluene to purify and centrifuged again. More details can be found in ref 18. A scanning electron microscopy (SEM) image of the powders shows that particles range in size from 1 to 100 μm and show a characteristic lamellar morphology (Figure 2).

Materials and Techniques. The alkanethiols (Aldrich) were used without further purification. All other reagents were acquired from general sources and used as received.

The following instruments were used: elemental analyzer, Fisons Instruments EA1108; X-ray diffractometer, Siemens D5000; X-ray photoelectron spectrometer, VG ESCALAB; differential scanning calorimeter, TA Instruments 2910; UV–vis spectrometer, Cary/Varian 5E; NMR spectrometer, Bruker DSX-300; infrared spectrometers, Mattson RS-1 and Bomem MB-100.

3. Results

Silver–alkanethiolates have been synthesized having chain lengths ranging from AgSC7 to AgSC18 (i.e. 7 to 18 total carbons). All materials have been extensively studied using IR spectroscopy. The AgSC12 material was chosen as a common reference, and a wide range of analyses were performed on it. Where required, other chain lengths were measured as well.

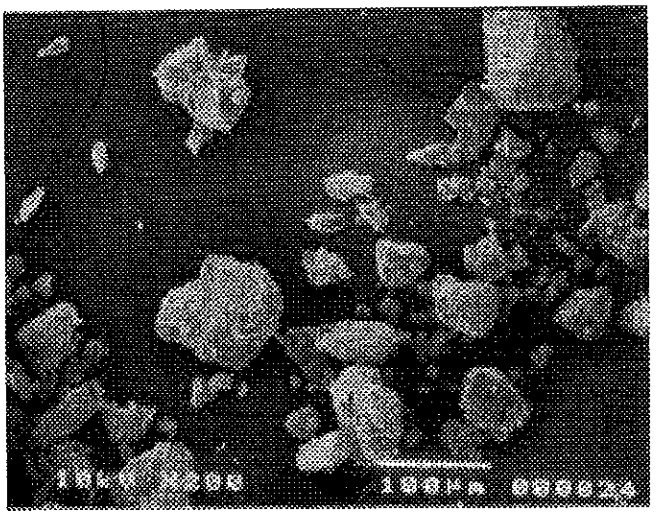

Figure 2. An SEM image of the AgSC12 material.

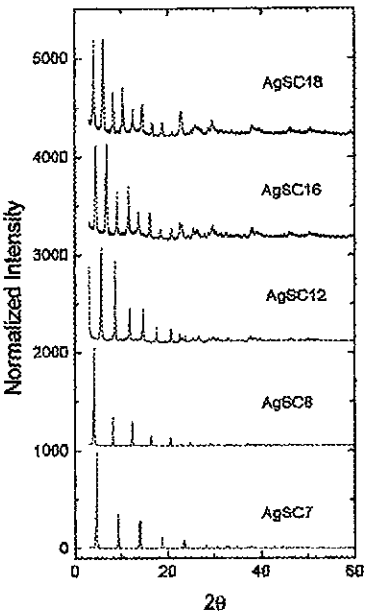

Figure 3. Powder XRD patterns from silver–alkanethiolate materials of various chain lengths, using Co Kα radiation (λ = 1.79021 Å).

(i) Elemental Analysis. The composition of the AgSC12 material was determined using elemental analysis (C 46.7%, H 8.2%, S 10.4%, all ±0.2%) and neutron activation analysis (Ag 36 ± 2%). This confirms that the material is of very high purity and that the stoichiometry is one thiolate group per silver atom (calculated C 46.6%, H 8.1%, S 10.4%, Ag 34.9%). This also shows that the synthesis procedure yields similar results to other methods, which also produced a precise 1:1 stoichiometry.[17]

(ii) X-ray Diffraction (XRD). An XRD analysis of all of the materials confirms that our method of synthesis produces the expected layered structure. The diffraction patterns are dominated by the (0k0) reflections (Figure 3), which can be used to determine the interlayer spacing. The interlayer spacing of each material is plotted in Figure 4 as a function of chain length. The linear correlation indicates that the materials share a common structure. Also plotted in the same figure are measured interlayer spacings taken from other references.[15–17] The agreement with the present results proves that the final structure

(18) Bensebaa, F.; Ellis, T. H.; Kruus, E.; Voicu, R.; Zhou, Y. *Can. J. Chem.*, in press.

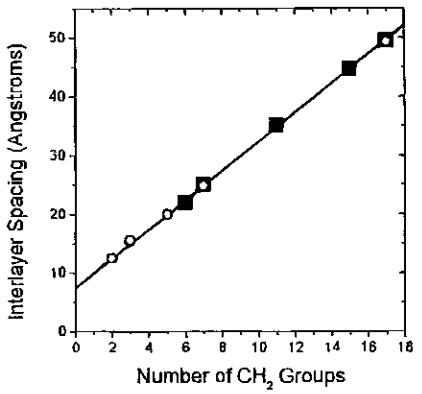

Figure 4. Measured interlayer spacings as a function of the number of methylene groups: (■) present work and (○) taken from refs 15–17. The slope of this plot, 2.48 ± 0.02 Å, is compared to the expected value for a linear chain to yield the tilt angle.

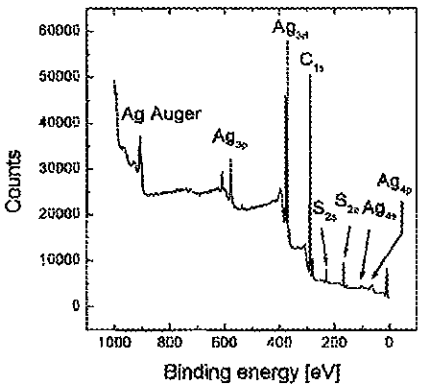

Figure 5. Survey XPS spectrum of the AgSC12 material.

is not sensitive to variations in the synthesis conditions, at least at these chain lengths.

Previous studies do not agree as to whether the remaining lines can be analyzed to determine the monoclinic unit cell.[15,17] There are number of lines, both broad and sharp, which are common to all chain lengths and are therefore probably related to the in-plane structure. Specifically, there is a sharp peak at 4.55 ± 0.03 Å for all chain lengths. [This can be compared to the measured lattice constants of thiolate monolayers on Ag(111), as determined by X-ray diffraction[4] (4.77 ± 0.03 Å), He diffraction[4] (4.67 ± 0.23 Å), and STM[7,8] (4.61 ± 0.15 Å and 4.40 ± 0.15 Å).]

(iii) X-ray Photoelectron Spectroscopy (XPS). Survey and high-resolution XPS scans are shown in Figures 5 and 6. These can be compared to XPS studies on thiolate monolayers, which are numerous (see ref 19 and references therein). The present results confirm minimal oxygen contamination. The narrow widths of the peaks are consistent with a single coordination geometry for each element. The $S2p_{3/2}$ and $Ag3d_{5/2}$ binding energy values (162.3 and 368.4 eV, respectively, as referenced to the 285.0 eV C1s peak) are typical for metal thiolate bonds.[20] However, the binding energy shift between Ag(0) and Ag(I) is too small to be used to determine the oxidation state of the metal.[20] The $S2p_{3/2}$ and $S2p_{1/2}$ peaks have been fit using a fixed 2:1 intensity ratio and a 1.2 eV separation. This is strong proof for a single bonding site for the sulfur atoms.

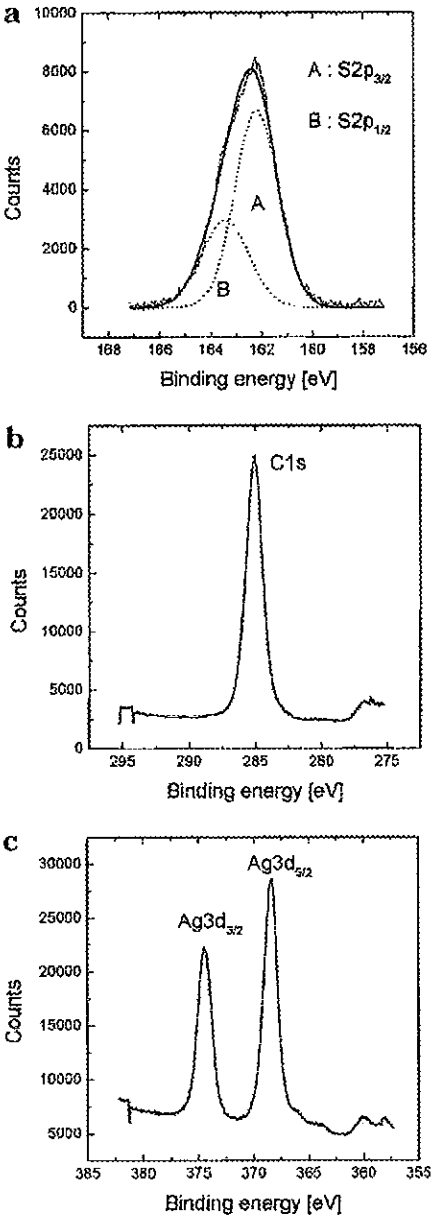

Figure 6. High-resolution XPS spectra of the AgSC12 material: (a) $S2p_{1/2}$ and $S2p_{3/2}$, (b) C1s, and (c) $Ag3d_{3/2}$ and $Ag3d_{5/2}$.

XPS measurements have also been performed on the other chain length materials. A linear relationship is found between the C/S intensity ratio as a function of the number of carbons, as shown in Figure 7. The intercept at $n = 1.4 \pm 1.0$ could reflect a slightly different environment for the carbons at the each chain end.

(iv) Electronic Structure. It has been shown by Natan and co-workers[17] that short-chain layered materials such as silver–butanethiolate can exist in two different forms, each having a 1:1 silver to thiolate stoichiometry. These two forms were denoted by T (for trans) and G (for gauche), on the basis of Raman spectroscopy showing gauche defects in the G form. A distinguishing feature of these two materials is the fact that T is white and G is bright yellow. This was quantified through the measurement of the electronic spectra. Our synthesis leads to solids with a slight pale yellow tinge, so the spectra of the AgSC12 material was measured in diffuse reflectance mode, as shown in Figure 8. The pronounced maximum in the spectrum at 340 nm is characteristic of the T form of silver–butanethiolate. In fact, as discussed below, the

(19) Castner, D. G.; Hinds, K.; Grainger, D. W. *Langmuir* **1996**, *12*, 5083–5086.

(20) Bensebaa, F.; Zhou, Y.; Deslandes, Y.; Kruus, E.; Ellis, T. H. *Surf. Sci.* **1998**, *405*, L472-L476.

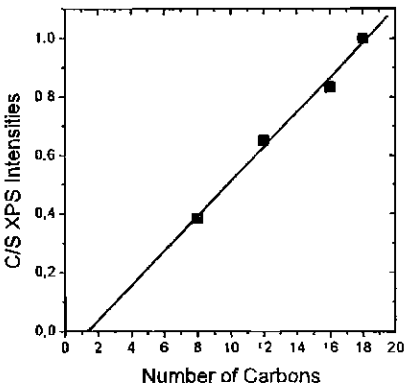

Figure 7. Normalized XPS intensity (C1s divided by $S2p_{3/2}$) as a function of chain length showing the expected linear correlation.

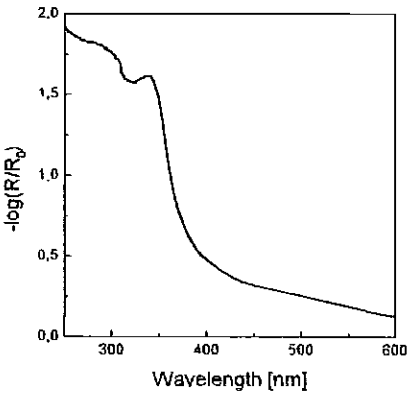

Figure 8. Electronic spectra of the AgSC12 material taken in diffuse reflectance mode.

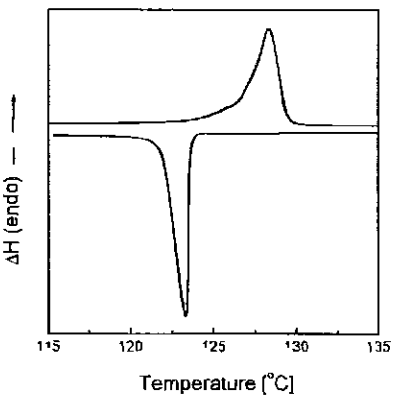

Figure 9. DSC traces for the AgSC12 material in both heating (upper trace) and cooling (lower trace) cycles. The ramping rate was 3 K/min.

electronic structure is indicative of the bonding geometry of the silver atom.

We have also synthesized silver–butanethiolate using our procedures, and this leads to a bright yellow material that has a maximum at 400 nm, so it is clearly the G form. It is therefore likely that longer chains show a tendency to form the T form.

(v) Differential Scanning Calorimetry (DSC). Phase transitions in these layered materials have been previously studied by Baena et al.[16] A typical heating and cooling scan for our AgSC12 material is shown in Figure 9. The well-defined phase transition occurring at 402 K (upon heating) has been assigned to a crystalline-to-micellar structural transformation.[16] The position of the transition was found to increase only slightly with chain length (5 K from AgSC8 to AgSC18). The transition

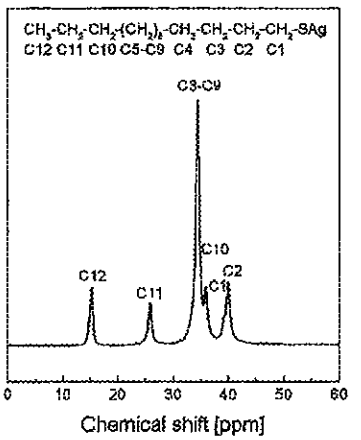

Figure 10. ^{13}C CP-MAS NMR spectrum of the AgSC12 material. Conditions: contact time, 5 ms; pulse delay, 4 s; spinning rate, 5 kHz; transients, 1282.

is reversible, and we have not detected any significant structural change in materials after having been cycled through the phase transition. We are currently studying the details of this transition using temperature-dependent FTIR and NMR. The initial results show that the chains remain highly conformationally ordered up to the transition, followed by a sharp increase in disorder at the transition. We have detected the presence of an interesting pretransition starting at low temperature.

(vi) Solid-State ^{13}C NMR. Cross-polarization magic angle spinning (CP-MAS) ^{13}C NMR measurements have been performed on the AgSC12 material, and the results are shown in Figure 10. The chemical shift of the midchain methylenes (34.4 ppm) indicates a very high degree of conformational order. The order is comparable to crystalline bulk alkanes, and higher than that observed with thiolate-capped nanoparticles (below 34 ppm), where a significant population of conformationally disordered chains was detected.[21] In the case of the latter, it was pointed out that the outermost methylene group (C11) must also contain gauche defects, because the shift of 24.2 ppm is well below that observed with solid alkanes (25.0). This group is observed at 25.8 ppm for the AgSC12 layered material, more proof of the high degree of conformational order throughout the chain.

A number of recent studies have shown that the formation of gold-thiolate bonds has a significant effect on the first two carbon atoms in the alkyl chain (C1 and C2). We assign the peak at 39.9 ppm and the shoulder at 39.2 ppm to C2 and C1, respectively. This compares to values of 40.1 (C1) and 39.4 (C2) measured by Badia et al.[22] for a gold–thiolate compound. We have reversed the assignment compared to that work based on a preliminary temperature-dependent study, which shows a larger variation for the 39.2 ppm peak. Although we have only measured the AgSC12 material, we suggest that the peaks at 40.5 and 39.3 measured by Fijolek et al.[17] for the trans form of silver–butanethiolate layered materials should be assigned to C2 and C1, respectively.

Badia et al.[22] argue that the magnitudes of these chemical shifts, particularly the large C1 shifts compared to thiols, are characteristic of the bonding in metal–alkylthiolate systems. They also point out that this is not the result of the metallic character of the metal atom. The present results confirm this, since the silver atoms in the

(21) Badia, A.; Gao, W.; Singh, S.; Demers, L.; Cuccia, L.; Reven, L. *Langmuir* **1996**, *12*, 1262–1269.

(22) Badia, A.; Demers, L.; Dickinson, F. G.; Morin, G.; Lennox, R. B.; Reven, L. *J. Am. Chem. Soc.* **1997**, *119*, 11104–11105.

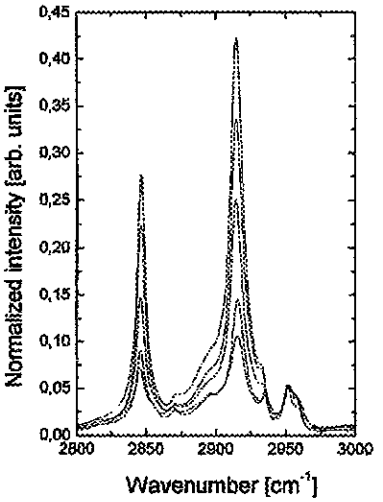

Figure 11. IR spectra (transmission mode) for, from bottom to top, AgSC7, AgSC8, AgSC12, AgSC16, and AgSC18 materials. The C–H stretching region is shown. Each spectra has been normalized to the r^-_b peak at 2952 cm^{-1}. Peak assignments are given in Table 1.

layered compounds are not likely to have a metallic character. Finally, it is interesting that the C1 and C2 peaks are difficult to observe on thiolate-capped gold nanoparticles, because the peaks are very broad. Both are located at 40.1 ppm, as determined by isotopic enrichment experiments.[22] The large widths were assigned to an inhomogeneous broadening which is the result of a distribution of bonding sites. The sharpness of these peaks in the case of layered materials indicates a single bonding site in these systems.

(vii) Infrared Spectroscopy. Infrared spectroscopy has been used extensively for the study of long alkyl chain systems, including thiolate monolayers on metal surfaces,[1,2] thiolate-capped nanoparticles,[11,13] phospholipid bilayers,[23] and bulk alkanes.[24–27] We have measured IR spectra in transmission mode on layered material dropcast onto NaCl windows, in reflection/absorption mode on particles partially aligned on flat gold mirrors, and directly on powders using photoacoustic (PA-FTIRS) spectroscopy. In all cases, the degree of order, as judged from the high number of clearly resolved peaks, is typical of highly ordered crystalline bulk alkanes. Such a high degree of order has never been observed in other metal–thiolate systems and allows a wealth of information to be obtained from the spectra.

Figure 11 shows the C–H stretching region. These spectra were obtained in transmission mode, on material that has been dropcast onto a NaCl window. The high degree of conformational order is best evidenced by the positions of the symmetric (d^+) and antisymmetric (d^-) CH_2 stretching peaks. Average values of 2847 ± 1 and 2916 ± 1 cm^{-1} for these peaks indicates an extremely high percentage of all-trans conformations. Disordered systems, such a liquid alkanes, display much higher values (2856 and 2928 cm^{-1}, respectively), which has been correlated to the higher number of gauche defects.[26] The

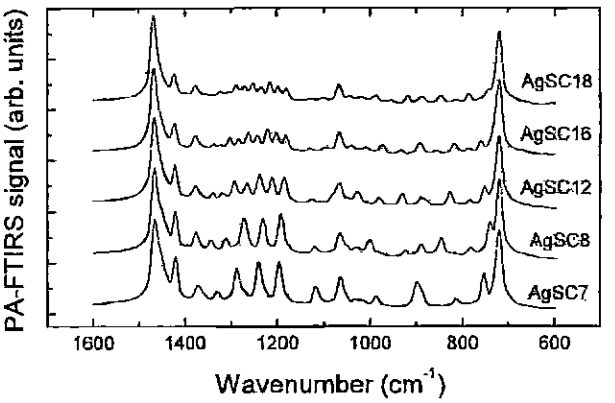

Figure 12. IR spectra (photoacoustic mode) for, from botton to top, AgSC7, AgSC8, AgSC12, AgSC16, and AgSC18 materials. The region shown contains the methylene wagging (W_k) and rocking–twisting (P_k) progressions, as well as other peaks. Peak assignments are given in Table 1.

values measured for the layered materials are similar to those of well-ordered solid *n*-alkanes.[25] In fact, at room temperature, the layered materials are one of the most conformationally ordered alkyl chain systems ever reported. The high degree of order is even observed in AgSC7, whereas all *n*-alkanes shorter than hexadecane are liquids at room temperature. The C–H stretching frequencies are even lower than the best results obtained for thiolate monolayers on metals.

Figure 12 shows the region between 700 and 1500 cm^{-1}, for materials ranging from AgSC7 to AgSC18, as measured directly on dried powders in photoacoustic mode. Similar results have been obtained in transmission mode. This is the first time that many of these features have been clearly resolved in a metal–thiolate system. It is clear that many peaks in this region vary with the chain length. All of the peaks can be straightforwardly assigned (see Table 1), and many result from CH_2 wagging and rocking–twisting modes. These modes are highly coupled and result in a progression of peaks, which is characteristic of an all-trans chain conformation. In fact, these peaks have previously been used as order parameters in other alkyl chain systems.[23]

4. Discussion

(i) Chain Orientation. On the basis of the XRD data, it is known that the overall structure of the layered materials is a central plane of silver atoms with thiolate chains extending out from both sides, as shown in Figure 1. Since the interlayer spacing is close to that expected for two extended thiolate chains, this rules out *complete* interdigitation between different layers. A linear relationship between the interlayer spacing and chain length is observed, with a slope of 2.48 ± 0.02 Å per pair of CH_2 segments (Figure 4). This is slightly smaller than one would expect for an all-trans chain which extends perpendicularly from the silver plane (2.54 Å per pair of CH_2 segments, based on a survey of a XRD data from a large number of ordered alkyl chain crystals). From this one can conclude that the chains are tilted by 12 ± 3 °from the normal. Such a value is in good agreement with the measured tilt angle of alkanethiolate monolayers on silver surfaces, where a tilt angle of 13 ± 2 °has been determined by a detailed analysis of the infrared spectrum.[2]

The intercept in Figure 4 is 7.4 ± 0.2 Å, which represents the thickness of the central layer (the separation between the C1 atoms on either side of the central plane) plus the separation between methyl groups of adjacent layers. It

(23) Senak, L.; Moore, D.; Mendelsohn, R. *J. Phys. Chem.* **1992**, *96*, 2749–2754.
(24) Snyder, R. G.; Schachtschneider, J. H. *Spectrochim. Acta* **1993**, *19*, 85–116.
(25) MacPhail, R. A.; Strauss, H. L.; Snyder, R. G.; Elliger, C. A. *J. Phys. Chem.* **1984**, *88*, 334–341.
(26) Snyder, R. G.; Strauss, H. L.; Elliger, C. A. *J. Phys. Chem.* **1982**, *86*, 5145–5150.
(27) Maroncelli, M.; Qi, S. P.; Herbert, L. S.; Snyder, R. G. *J. Am. Chem. Soc.* **1982**, *104*, 6237–6247.

Table 1. Mode Assignments for the Silver–Alkanethiolate Layered Materials[a]

wavenumber	intensity	assignment	wavenumber	intensity	assignment	wavenumber	intensity	assignment
				AgSC7				
721	s	P_1	1196	m	W_1	2846	s	d^+
755	m	P_3	1240	m	W_2	2869	w	r^+
814	w	P_4	1287	m	W_3	2896	sh	FR
899	m	β+P_5	1329	w	W_4	2916	s	d^-
988	w	P_6	1371	w	U+W_5	2926	w	FR
1065	m	X	1421	m	δ_s	2952	m	r^-_b
1117	w	R_2	1466	s	δ	2960	w	r^-_a
				AgSC8				
720	s	P_1	1120	w	R_2	1467	s	δ
741	m	P_3	1193	m	W_1	2847	s	d^+
782	vw	P_4	1232	m	W_2	2872	w	r^+
847	w	P_5	1273	m	W_3	2896	sh	FR
890	w	β	1312	w	W_4	2916	s	d^-
926	vw	P_6	1343	w	W_5	2936	w	FR
1002	w	P_7	1376	w	U+W_6	2953	m	r^-_b
1066	m	X	1421	m	δ_s	2959	w	r^-_a
				AgSC12				
720	s	P_1	1067	w	x	1377	w	U
724	sh	P_3	1081	vw	R_3	1423	m	δ_s
734	sh	P_4	1127	vw	R_2	1469	vs	δ
753	w	P_5	1186	m	W_1	2847	vs	d^+
784	vw	P_6	1212	m	W_2	2872	w	r^+
828	w	P_7	1240	m	W_3	2895	sh	FR
879	vw	P_8	1267	m	W_4	2916	vs	d^-
891	w	β	1293	m	W_5	2934	sh	FR
932	w	P_9	1318	vw	W_6	2953	s	r^-_b
983	vw	P_{10}	1339	vw	W_7	2958	sh	r^-_a
1028	w	P_{11}	1356	w	?			
				AgSC16				
721	s	P_1	1097	vw	R_3	1377	w	U
761	w	P_7	1129	vw	R_2	1424	m	δ_s
786	vw	P_8	1183	w	W_1	1468	s	δ
818	w	P_9	1202	w	W_2	2847	vs	d^+
856	vw	P_{10}	1222	m	W_3	2872	w	r^+
893	w	β	1243	w	W_4	2894	sh	FR
936	vw	P_{12}	1263	w	W_5	2915	vs	d^-
974	w	P_{13}	1283	w	W_6	2934	sh	FR
1010	vw	P_{14}	1303	w	W_7	2952	s	r^-_b
1040	vw	P_{15}	1321	vw	W_8	2961	sh	r^-_a
1067	w	X	1338	vw	W_9			
				AgSC18				
721	s	P_1	1068	w	X	1322	vw	W_9
745	w	P_7	1102	vw	R_3	1378	w	U
764	sh	P_8	1129	vw	R_2	1424	m	δ_s
787	w	P_9	1182	w	W_1	1469	vs	δ
814	vw	P_{10}	1199	w	W_2	2847	vs	d^+
848	w	P_{11}	1217	w	W_3	2872	w	r^+
889	w	β+P_{12}	1235	w	W_4	2894	sh	FR
919	w	P_{13}	1253	w	W_5	2915	vs	d^-
954	vw	P_{14}	1271	w	W_6	2934	sh	FR
989	w	P_{15}	1288	w	W_7	2952	s	r^-_b
1021	vw	P_{16}	1306	vw	W_8	2961	sh	r^-_a

[a] Peak positions and intensities were obtained from transmission IR spectra. They correlate very well with the photoacoustic results, except that the latter were taken with lower resolution, and some strong peaks were saturated. Abbreviations are as follows: vs, very strong; s, strong; m, medium; w, weak; vw, very weak; sh, shoulder. Nomenclature conforms to refs 24 and 25.

has been suggested by Dance et al.[15] that the latter may interdigitate to a small extent, so it is difficult to estimate any individual distances from this one number. It would, for example, be useful to determine the height of a sulfur atom above the silver plane, to learn about the bonding coordination, or to determine the degree of "buckling" of the silver plane. However, we can only say that any proposed structural model will have to respect the total layer thickness determined by XRD.

(ii) Chain Conformation. The above interpretation assumed fully extended, all-trans chains, and evidence for this comes from both the NMR data (as discussed above) and the IR data. The very low frequencies of the methylene stretching modes indicates a very low number of gauche defects. A second test is the observation of the band progressions between 700 and 1500 cm^{-1}. Senak et al.[23] have used these peaks as a measure of order and have shown a strong correlation to the methylene stretching frequencies. Snyder et al.[24] have shown that a simple coupled oscillator model can be used to assign all wagging modes from different chain lengths. Given a linear array of m identical coupled oscillators, it can be shown that the frequencies vary directly with the phase difference between adjacent oscillators, as given by

$$\varphi_k = \frac{k\pi}{m+1} \qquad k = 1, 2, 3, ..., m$$

Table 1 shows a summary of all of the wagging peaks (W_k), and Figure 13 shows that all of these peaks fall close

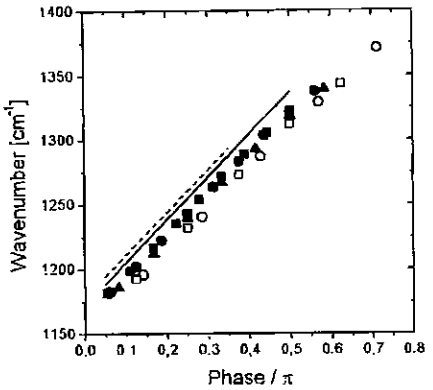

Figure 13. Individual peak positions of the methylene wagging progression (W_k) are plotted as a function of phase shift (see text): (○) AgSC7; (□) AgSC8; (▲) AgSC12; (●) AgSC16; and (■) AgSC18. Also shown are the best fits to a similar analyses performed for: (solid line) bulk alkanes from ref 24 and (dashed line) lipid bilayers from ref 23.

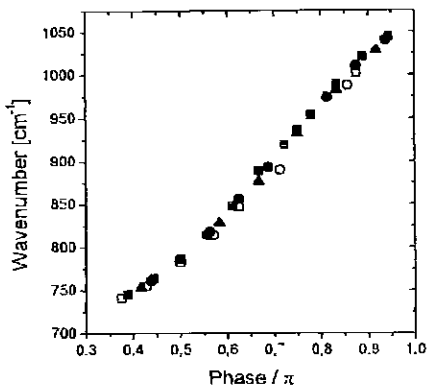

Figure 14. Individual peak positions of the methylene rocking–twisting progression (P_k) are plotted as a function of phase shift (see text): (○) AgSC7; (□) AgSC8; (▲) AgSC12; (●) AgSC16; and (■) AgSC18.

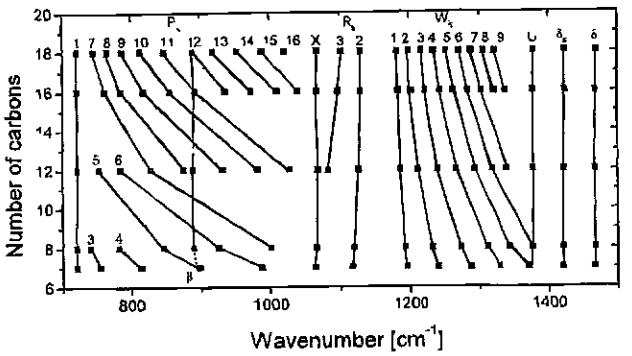

Figure 15. A summary of the progressions of all peaks in the region between 700 and 1500 cm^{-1}. Individual peak assignments are shown, and the frequencies are given in Table 1. This type of plot emphasizes the regularity of the peak positions.

Table 2. Spacing of the Peaks in the Wagging Band Progression as a Function of the Number of Methylene Oscillators

no. of CH_2 groups	*n*-alkanes[a]	W_3-W_1 (cm^{-1})	layered materials	W_3-W_1 (cm^{-1})
4	*n*-C_6	111		
5	*n*-C_7	100		
6	*n*-C_8	93	AgSC7	91
7	*n*-C_9	83	AgSC8	80
8	*n*-C_{10}	75		
9	*n*-C_{11}	66		
10	*n*-C_{12}	62		
11	*n*-C_{13}	56	AgSC12	53
12	*n*-C_{14}	52		
13	*n*-C_{15}	49		
14	*n*-C_{16}	44		
15	*n*-C_{17}	42	AgSC16	39
16	*n*-C_{18}	41		
17	*n*-C_{19}	32[b]	AgSC18	35

[a] Taken from ref 24. [b] This value does not follow the expected pattern, suggesting that the peak assignments may not be accurate.

to a universal curve. Also shown are the best fits to similar wagging progressions measured for solid alkanes[24] and phospholipid bilayers.[23] The slopes are similar for all three systems. The frequencies observed in the layered systems are systematically lower. The two shorter chains (AgSC7 and AgSC8) are also systematically lower than the longer chains.

Another series of peaks can be easily assigned as belonging to the rocking–twisting progression (P_k), giving rise to the curve shown in Figure 14. The most intense peak in this series (P_1) is observed at 721 ± 1 cm^{-1} for all chain lengths. Once again all of the peaks belonging to this series lie on a universal curve when analyzed using the simple coupled oscillator model, which assumes an all-trans structure. A third series, the carbon–carbon stretching progression (R_k), follows a less straightforward trend. Figure 15 shows the peak positions of all of the measured peaks located between 700 and 1500 cm^{-1}. The carbon–carbon stretching peaks are known to fall between 950 and 1150 cm^{-1}. However, they fall into two regions. As stated by Snyder and Schachtschneider,[24] there is clear regularity above 1065 cm^{-1} (known as region A) in the case of solid *n*-alkanes, which is true also for the layered compounds. In the lower wavenumber region B, the patterns are more subtle and we have not assigned peaks from this progression in this second region. Apart from these few peaks, all of the other peaks seen in Figure 12 can be straightforwardly assigned, and in some cases, useful information can be extracted from them.

The intense peak observed at 1468 ± 1 cm^{-1} for all chain lengths is assigned to the methylene symmetric bending mode (δ). In addition, there is always a clearly resolved second peak at 1422 ± 2 cm^{-1}, which has been assigned to the bending mode of the methylene group located next to the sulfur atom (δ_s).[11] It has previously been observed as shoulder in measurements of thiolate-capped nanoparticles. Due to the well-resolved peaks, we can clearly see that its intensity decreases relative to the main bending peak as the chain length increases, which supports its assignment. Therefore, the first methylene group in the chain is clearly different from the others. Despite this, the methylene wagging modes can still be treated as "identical" to the rest of the chain, at least with respect to the coupled oscillator model. For example, if the AgSC12 material was treated as having only 10 identical methylene groups rather than 11, then the data points in Figure 13 would lie far below the curves that characterize solid *n*-alkanes and lipid bilayers. Another proof of this is the spacing between peaks in the wagging progression. As shown in Table 2, the difference between the W_1 and W_3 peaks decreases continuously with increasing chain length for solid *n*-alkanes. (W_2 is not used for this calculation because it is not observed in the even *n*-alkanes, for symmetry reasons.) Following this trend, it is clear that the layered materials behave in a similar fashion as linear alkanes with the *same number of methylene groups*. The slightly different environment of the first methylene group does not change this, or, in

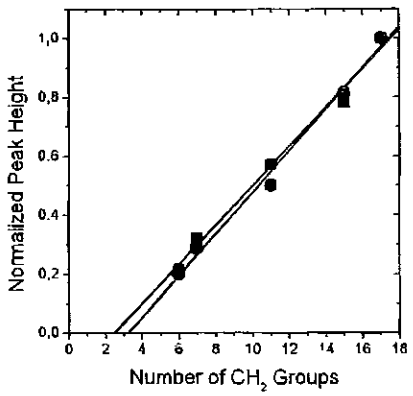

Figure 16. Normalized intensities of the methylene stretching peaks as a function of chain length: (■) antisymmetric mode d^- and (●) symmetric mode d^+. Each peak has been normalized to the corresponding r^-_b peak at 2952 cm^{-1}.

other words, the peaks in these progressions are not sensitive to minor perturbations.

Other peaks that do not shift in frequency are assigned to the methyl symmetric bending, or umbrella mode (U) at 1377 ± 1 cm^{-1} and the in-plane methyl rocking mode (β) at 889 ± 1 cm^{-1}. Less certain is the relatively intense peak observed at 1067 ± 2 cm^{-1}. The spectrum of the solid *n*-alkanes often have a peak near this value, which represents the upper limit of the B region of the carbon–carbon stretching (R) progression. An alternative explanation is that this is vibrational mode of a defect. Maroncelli et al. have observed such a mode at 1078 cm^{-1}.[27] This assignment is less likely, given the significant difference in wavenumbers, and the fact that we do not observe the other peaks which are characteristic of this same defect (1341, 1164, 955, and 873 cm^{-1}).[27]

We conclude this section with a discussion on the peak intensities. First, it is worth noting that there is no even/odd intensity variation in the wagging band progression, in contrast to the behavior of the solid *n*-alkanes.[24] This lack of variation was also observed with phospholipid bilayers[23] and explained in terms of the broken symmetry. Next, as shown in Figure 16, the intensities of the methylene stretching peaks (d^+ and d^-) follow a linear increase with chain length, once they have been normalized to the r^-_b peak. This curve also indicates that the first two or three methylene groups do not contribute to the intensity at the wavenumber of the measurements. A similar result has been observed in the case of thiolate SAMs on Ag(111),[1] except that the extrapolation to zero intensity occurs between four and five methylenes. In the case of the layered materials it is certain that this effect is not related to dipole selection rules specific to metal surfaces. It is more likely that there is a significant frequency shift for the first methylenes. A recent deuterium enrichment experiment showed such a shift for the first methylene in a thiolate-capped gold nanoparicles (2123 cm^{-1} compared to 2088 cm^{-1} for the rest of the chain, for the d^+ mode).[13]

(iii) Structural Model in the Plane. In the absence of a detailed XRD determination, the structure of the central plane of the bilayer can only be inferred from indirect evidence. Previously proposed models are best described as a distorted hexagonal lattice of alternating Ag and S atoms. Fijolek et al. have proposed a more detailed model for silver butanethiolate layered compounds which takes into account the two different forms which have been isolated for this short chain system (T and G).[17] Our present results for longer chain systems

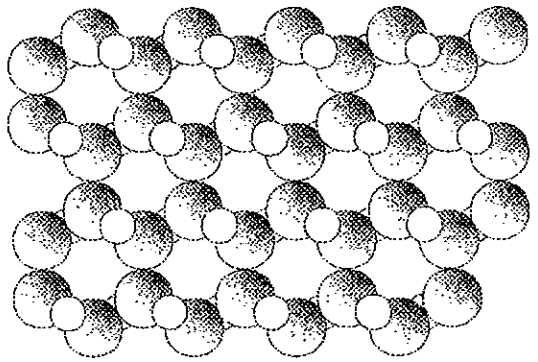

Figure 17. A proposed model for the in-plane structure of metal–alkanethiolate layered materials. The metal atoms are represented by shaded circles, and the sulfur atoms are white circles. This model differs in some details from previous models.[15,17] By placing the metal atoms in a hexagonal arrangement, the sulfur atoms can adopt a digonal bonding arrangement while at the same time templating a close-packed geometry for the alkyl chains (not shown).

are not fully consistent with these structures, for two reasons. First, the high degree of conformational order in the alkyl chains suggests a close-packed, all-trans environment, which is inconsistent with previous models. Second, the UV–vis spectra of our compounds has a peak maximum at 340 nm, which, based on numerous studies of inorganic compounds, is consistent with a digonal S–Ag–S environment, rather then the proposed trigonal arrangement.[28]

An alternative model can be proposed, as shown in Figure 17, which is motivated by the structure of close-packed thiolate monolayers on (111) hcp metal surfaces. In such systems, there is one thiolate group for every three surface metal atoms. A bilayer has thiolate chains on either side of the central layer, which results in a "$^2/_3$ coverage" of metal atoms, to preserve the measured stoichiometry. A hexagonal arrangement of Ag atoms in the central layer fulfills all requirements. By placing the thiolate groups in "bridge sites", it is also possible to achieve the required digonal coordination. We have suggested that this model can apply to both silver and copper layered materials.[18]

The above model also allows the silver atoms to come into close contact with each other, as close as they would on the surface of solid silver. It has been observed by Dance et al.[28] that the silver–silver distance in many inorganic compounds of the form $(AgSR)_n$ is about 2.9 Å, which is identical to the interatomic spacing in bulk silver. However, in the latter case there exist strong metal–metal bonds, whereas it is believed that the spacing in the inorganic compounds results from the repulsive interaction between *nonbonded* silver atoms. According to this interpretation, it is purely coincidental that the equilibrium spacing between Ag(0) atoms is equal to the equilibrium spacing between Ag(1) atoms.

(iv) Relevance to SAMs on Ag(111) Surfaces. It is informative to compare and contrast the layered compounds and thiolate monolayers on metal surfaces. In the former, the silver layer is composed of only Ag(1) atoms, whereas the oxidation state of metal atoms on the silver surface is unknown. More importantly, the layered compounds allow for the stable linear S–Ag–S coordination preferred in inorganic compounds,[28] whereas thiolate monolayers can accommodate only S–Ag_n bonds, depending upon the bonding site. Despite these differences, the

(28) Dance, I. G.; Fitzpatrick, L. J.; Rae, A. D.; Scudder, M. L. *Inorg. Chem.* **1983**, *22*, 3785–3788.

two systems share many common properties, such as similar tilt angles of the methylene chains.

Closely related to the issue of tilt angles is the fact that SAMs on Au(111) are commensurate with the underlying lattice, whereas for Ag(111) they are incommensurate.[4,7,8] There must be a driving force for the incommensurate structure, and it is possible that this is related to the high degree of order and the stability of the layered materials. Since monolayers and bilayers share the same tilt angle they most likely have a similar packing density. It should also be pointed out that bilayers may be formed during the preparation of SAMs on silver surfaces. It has been noted that prolonged exposure to thiol solutions can degrade the surface, and silver can be detected in the solutions.[7,8] Walczak et al. reported that thick multilayer films were grown when very short chain thiols were used in the preparation of SAMs on Ag(111).[1] It has been reported that multilayer films can be grown on copper surfaces,[29] and we have recently shown that copper layered materials are very similar to silver ones.[18] All this suggests that great care must be taken during the preparation of SAMs on silver and copper surfaces. One can even speculate that the elevated islands seen in the STM images of Dhirani et al.[8] could be bilayer islands. Since monolayers and bilayers have very similar structures, it will be difficult to distinguish between them using most techniques.

(29) Kellor, H.; Simak, P.; Schrepp, W.; Dembowski, J. *Thin Solid Films* **1994**, *244*, 799.

5. Conclusion

Silver−alkanethiolate layered materials have been characterized by a wide range of experimental techniques. The alkyl chains are found to tilt by 12 ° with respect to the surface normal. There are thus likely to be similarities between the layered materials and the incommensurate thiolate monolayers previously observed on Ag(111), which have a similar tilt angle. The thermal stability and the degree of chain conformational order in the layered materials is found to be the highest of any alkanethiolate system yet studied. The order extends even to the outermost methylene group at room temperature. The infrared spectra of these materials are particularly rich in information, and it has been possible to provide a comprehensive assignment of individual features. These measurements provide a useful reference point in study of all alkanethiolate self-assembled systems.

Acknowledgment. The authors thank the Natural Sciences and Engineering Research Council of Canada for funding. F.B., R.V., and Y.Z. acknowledge the Group de Recherche en Physique et Technologie des Couche Minces for scholarships. We would also like to thank the following people: Minh Tan Phan Viet, Robert Mayer, Chantal Paré, and Michel Lafleur (NMR), Suzie Poulin (XPS), Karim Faïd (DSC), and Guillaume Bussière and Christian Reber (UV−vis).

LA980718G